Construction and Building Materials 187 (2018) 760–772

Contents lists available at ScienceDirect

Construction and Building Materials

journal homepage: www.elsevier.com/locate/conbuildmat

Corrosion inhibition of carbon steel by dipotassium hydrogen phosphate in alkaline solutions with low chloride contamination

A. Mohagheghi, R. Arefinia *

Chemical Engineering Department, Faculty of Engineering, Ferdowsi University of Mashhad, Mashhad, Iran

HIGHLIGHTS

- There was a critical [DKP]/[Cl^-] ratio to passivate the carbon steel surface.
- The impact of phosphate on the stability of the passive film depends on the [Cl^-]/[OH^-] ratio.
- In a mildly alkaline solution, phosphate inhibits pitting and uniform corrosions.
- In a highly alkaline solution, phosphate is efficient to uniform corrosion.
- Phosphate acts as an anodic inhibitor through forming a duplex layer passive film.

ARTICLE INFO

Article history:
Received 23 February 2018
Received in revised form 6 July 2018
Accepted 25 July 2018

Keywords:
Carbon steel
Pitting corrosion
Uniform corrosion
Concrete
Phosphate
Passive film

ABSTRACT

This work deals with the corrosion inhibition of carbon steel by dipotassium hydrogen phosphate (DKP) in both mildly and highly alkaline solutions (pH 8 and 12) contaminated with low levels of chloride (1–5 mmol L^{-1}). To this end, the electrochemical methods of potentiodynamic polarization, electrochemical impedance spectroscopy (EIS) together with different surface analysis methods including scanning electron microscopy (SEM), energy dispersive spectroscopy (EDS) and Raman spectroscopy were employed. In mildly alkaline solution, the [DKP]/[Cl^-] ratio should be greater than the critical value (3.7) to form a stable passive film on the metal surface; additionally, the best inhibition against uniform corrosion was achieved at [DKP]/[Cl^-] = 5.5, while the passive film resistance to pitting resistance continuously improved as the [DKP]/[Cl^-] ratio increased. The effect of chloride concentration on the characteristic of passive film was described by a logarithmic relationship. In highly alkaline solution, addition of 11 mmol L^{-1} DKP has a significant effect on uniform corrosion. The surface analysis methods demonstrated the formation of a duplex layer on the metal surface composed of an inner layer of iron oxides and an outer layer of iron phosphate complexes mainly as $FeHPO_4$ and $Fe_3(PO_4)_2$.

1. Introduction

Inhibitors are promising chemical compounds that are used to suppress the corrosion of metals in aqueous solutions [1]. Phosphate compounds as inorganic inhibitor [2–5] and antiscalant material [6] are particularly popular due to their low cost and low toxicity. Different phosphate compounds such as disodium hydrogen phosphate (Na_2HPO_4) [1,3], disodium mono fluoride phosphate (Na_2PO_3F) [7,8], zinc phosphate [9], and lithium zinc phosphate [10] have been used to control the corrosion process especially against localized corrosion induced by aggressive anions like chloride.

The inhibition mechanism of phosphate has been well investigated and documented [11,12]; however, it is somehow controversial [13,14]. Some researchers have found that phosphate is an anodic inhibitor which functions through the formation of a passive film on the metal surface [3,15], while cathodic or mixed inhibition mechanism has been also reported [5,16]. In the case of anodic protection for steel in an alkaline solution, the passive film is mainly made of two parts [15]: the inner layer of iron oxides mainly involving magnetite (Fe_3O_4) or/and maghemite (Fe_2O_3) [17] as well as the outer layer of iron phosphate such as $FeHPO_4$, $Fe_3(PO_4)_2$ and $FePO_4$. The presence of phosphate compounds within the structure of the outer layer has been confirmed before using different surface analysis methods such as XPS and AES analysis [15], Raman spectra [5], ellipsometric [11], and x-ray [18]. Nishimura et al. [19] have studied the breakdown mechanism of passive film on the iron surface in the phosphate and borate

* Corresponding author.
E-mail address: arefinia@um.ac.ir (R. Arefinia).

https://doi.org/10.1016/j.conbuildmat.2018.07.181
0950-0618/

solutions containing high chloride content at pH 8.42 and 11.5. They reported that the ion selectivity of the passive film has an important effect on the nucleation and growth of pits.

Phosphate compounds can be efficiently employed to control the pitting corrosion of steel reinforcement in concretes which is supported by the finding of so many studies in the literature [20–22]. The primary focus of these studies is on the competitive adsorption between phosphate and chloride ions on the steel surface in various simulated concrete pore solutions [14,23,24]. Yohai et al. [5,13,25,26] have extensively investigated the inhibition mechanism of phosphate by varying $[PO_4^{3-}]/[Cl^-]$ ratio and $[Cl^-]/[OH^-]$ ratio in simulated pore solutions of concretes. They have pointed out the significant effect of phosphate and its dosage relative to that chloride on the pitting corrosion resistance.

In this field, the primary concern of most studies has been on the evaluation of the phosphate inhibition in synthetic solutions with a high-chloride concentration and commonly at high pH values around 12. However, chloride contamination is controlled by the diffusion of chloride ions within concrete pores and, consequently, high chloride contamination probably occurs after a long time exposure. Before this, it is reasonable to state that the corrosion within the pore solution develops at low chloride contamination. Recently, Nahali et al. [27] have studied the influence of phosphate ions on the diffusion coefficient of chloride ions in mortar and they have found a low chloride concentration within the cells simulating concrete pores even after 100 days of immersion at pH = 12. Nevertheless, a few studies have investigated the effect of varying phosphate and chloride concentration on the phosphate inhibition at low chloride contamination and at different pH values. These factors may cause significant effects on both uniform and pitting corrosion of steel.

In this study, the inhibitive effect of dipotassium hydrogen phosphate (DKP, K_2HPO_4) on both uniform and pitting corrosion of carbon steel was investigated in mildly alkaline solutions (pH of about 8.8) with low levels of chloride contamination by varying phosphate and chloride concentrations. In addition, the effect of phosphate at a certain concentration on the uniform and pitting corrosion of carbon steel was studied in a highly alkaline solution (pH 12). The selected conditions correspond to the cooling waters and the early stage of corrosion in the concrete pores. Electrochemical methods including potentiodynamic polarization and electrochemical impedance spectroscopy (EIS) together with surface analysis techniques of the scanning electron microscopy (SEM), energy dispersive spectroscopy (EDS) and Raman spectroscopy were employed to study the phosphate inhibition mechanism at the selected conditions of this work.

2. Experimental

2.1. Materials and electrolyte

Dipotassium hydrogen phosphate (DKP), as the inhibitor, was prepared from Merck Co. as an analytical grade. The chemical composition of carbon steel A106 as the working electrode is presented in Table 1. The specimens were mounted with epoxy when the remaining surface area was 1.0 cm^2 as a square shape. In prior electrochemical tests, the surface of specimens was abraded by 300, 600, 1200, and 2000 grades of emery paper, degreased and rinsed with acetone and distilled water, respectively, and then immediately dried to prevent any corrosion occurrence.

Table 2
Variation of solution pH with DKP concentration.

DKP concentration (mmol L^{-1})	Blank	7	11	17	23
pH	7.78	8.73	8.80	8.82	8.89

The inhibition mechanism of phosphate ions was studied in a 2 mmol L^{-1} chloride solution at different concentrations (0, 7, 11, 17 and 23 mmol L^{-1}) of phosphate and at room temperature (25 ± 2 °C). In addition, the effect of chloride concentration including 0, 1, 2, 3 and 5 mmol L^{-1} on the corrosion of carbon steel was quantitatively evaluated in an 11 mmol L^{-1} phosphate solution at room temperature. The increase in phosphate concentration has a negligible effect on the solution pH because of the buffer nature of DKP, as demonstrated in Table 2.

2.2. Electrochemical measurements

All the electrochemical measurements were performed using an Autolab potentiostat/galvanostat (PGSTAT 302N) in a glass cell with three electrodes: a saturated calomel electrode (SCE) as reference, a graphite rod of large area as counter electrode and a mounted carbon steel as working electrode. In addition, all electrochemical measurements were repeated at least three times until a good reproducibility was observed.

The potentiodynamic polarization test was performed from −400 mV below OCP to reach the pitting or oxygen evolution potential at the scan rate of 0.5 mV/s. Since the corrosion state may be as active, active-passive and completely passive, in each case, the value of corrosion current density (i_{corr}) was determined using known methods. For the active state, i_{corr} was obtained by the application of Tafel extrapolation at potentials about 100 mV far from the E_{corr} where a linear behavior (Tafel region) is observed, while, for the passive state, corrosion current density has in fact the same meaning as passive current density (i_{pass}). Therefore, for the systems with an active-passive transition state, both corrosion current and passive current (i_{corr}/i_{pass}) were determined. For all the systems, determination of cathodic Tafel slope (β_c) may be still useful in analyzing the reduction behavior of electrolyte components. It should also be noted that the value of anodic Tafel slope (β_a) is meaningful only for the active or active/passive states of corrosion and not for the completely passive. Moreover, the value of passive potential (E_{pass}) was considered equal to the corrosion potential (E_{corr}) for completely passive systems, while for active/passive systems, E_{pass} was determined from the beginning of the passive region in polarization curves where the current density was approximately constant by sweeping the potential.

The electrochemical impedance spectroscopy (EIS) was conducted at an amplitude perturbation of 10 mV versus OCP over the frequency range of 10 kHz–10 mHz. The EIS analysis was made through fitting the recorded spectra to the suitable equivalent circuits in Zview software.

2.3. Weight loss measurements

The inhibition effect of DKP on the corrosion of carbon steel in the long term was evaluated by measurement of weight loss during 45 days of immersion at room temperature in aerated conditions according to ASTM D 2688. The working specimens had a

Table 1
Chemical composition of carbon steel A106.

Elements	Fe	C	Mn	P	S	Si	Cr	Cu	Mo	Ni	V
Composition (wt. %)	balance	0.35	1.06	0.04	0.04	0.10	0.40	0.40	0.15	0.40	0.08

rectangular shape with a dimension of 1 × 1 × 0.5 cm. The weight loss tests were conducted in a 2 mmol L^{-1} chloride solution at 0 and 11 m mmol L^{-1} DKP. In each case, the weight of two specimens was measured prior and after exposure to the corrosive solution. At the end of immersion, the samples were withdrawn and the corrosion products deposited on the specimens were removed by immersion in HCl 1 mmol L^{-1} and, then, neutralized and rinsed, first with a saturated Na_2CO_3 solution and then with distilled water.

2.4. Surface analyses

The effect of chloride and phosphate concentration on the corrosion state of metal surface was investigated using the scanning electron microscopy (SEM, LEO 1450VP) and the elements present in the pitted points were determined by energy dispersive spectroscopy (EDS). SEM/EDS tests were carried out after the polarization test over the carbon steel surface until the pitting potential was achieved.

Raman spectroscopy was performed with an AvaRaman-785 TEC with a 785 nm laser wavelength, exposure time 15 s, and laser power 500 mW. Ex-situ Raman spectroscopy technique was employed to study the passive film formed in the metal/solution interface. This test was performed after the polarization test of the sample in a 2 mmol L^{-1} chloride + 11 mmol L^{-1} DKP solution. Raman data were collected at both pitting attack locations and zones without pits.

3. Results and discussion

3.1. Effect of phosphate concentration

3.1.1. Potentiodynamic polarization

Fig. 1 shows the polarization curves for carbon steel in mildly alkaline solutions (with a pH of about 8.8) with a 2 mmol L^{-1} chloride concentration and at different DKP concentrations: 0, 7, 11, 17 and 23 mmol L^{-1} corresponding to [DKP]/[Cl^-] ratios of 0, 3.5, 5.5, 8.5 and 11.5, respectively. It is obvious that the corrosion behavior is in active state in the solution without phosphate and at 7 mmol L^{-1} ([DKP]/[Cl^-] =3.5) it changes to an active-passive transient state, while a completely passive behavior is achieved by further addition of DKP. These observations suggest that the [DKP]/[Cl^-] = 3.5 can be considered as a critical ratio at which the higher phosphate content could passivate the surface of carbon steel at selected conditions here and, thus, the less value of [DKP]/[Cl^-] may lead to serious corrosion of carbon steel.

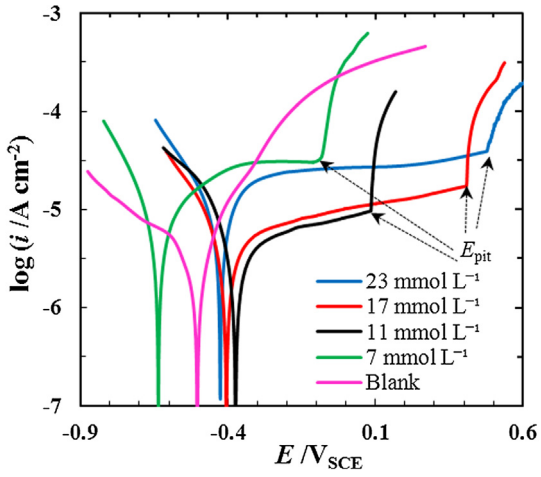

Fig. 1. Effect of DKP concentration on the potentiodynamic polarization curves for carbon steel in a mildly alkaline solution with 2 mmol L^{-1} chloride at 25 °C. Scan rate: 0.5 mV s^{-1}.

The average values of polarization parameters obtained from Fig. 1 are presented in Table 3 where the inhibition efficiency (IE) was calculated using the following equation:

$$IE\% = \left(\frac{i^0_{corr} - i_{corr}}{i^0_{corr}}\right) \times 100 \quad (1)$$

where i^0_{corr} and i_{corr} are the corrosion current density of carbon steel in the absence and presence of phosphate, respectively.

It is found from Table 3 that when 7 mmol L^{-1} DKP is added to the solution, corrosion potential (E_{corr}) shifts to more negative values, corrosion current density (i_{corr}) slightly increases from 7.9 to 9.2 μA cm^{-2}, and a passive state is achieved only at high applied potentials associated with high passive current density (i_{pass}). These evidences suggest that the addition of 7 mmol L^{-1} DKP stimulates dissolution of carbon steel and phosphate cannot make a passive film on the metal surface at E_{corr}.

When phosphate dosage increases from 7 to 11 mmol L^{-1}, a passive state is established at E_{corr}, which has the same meaning as E_{pass}. Moreover, E_{pass} moves in the positive direction and i_{corr} significantly decreases. These behaviors clearly suggest the anodic inhibition mechanism of phosphate. By further addition of phosphate up to 23 mmol L^{-1} ([DKP]/[Cl^-] = 11.5), E_{pass} shifts negatively and i_{pass} increases, showing the increase in the rate of uniform corrosion. At the same time, pitting potential (E_{pit}) and passivation region ($E_{pit} - E_{pass}$) considerably increase, which support the higher passive film resistance to pitting corrosion.

Table 3 shows that the absolute value of cathodic slope (β_c) continuously decreases as phosphate concentration increases, which is attributed to the facilitation in the reduction reaction. This behavior could be considered an advantage in the protection mechanism of passivating anions like phosphate species. In parallel, the increase of β_a by addition of 7 mmol L^{-1} DKP indicates the tendency of phosphate to passivate the metal surface; however, the insufficient concentration of phosphate species relative to that of chloride ion (low ([DKP]/[Cl^-]) is a limiting factor.

In this regard, Dhouibi et al. [28] have studied the effect of [DKP]/[Cl^-] on steel corrosion in concrete solutions with a high level of chloride contamination at pH 11.4. They proposed that [DKP]/[Cl^-] = 0.6 is a critical value at which lower- and higher-value, phosphate acts as a cathodic and anodic inhibitor, respectively. On comparing with the critical ratio of [DKP]/[Cl^-] = 5.5 obtained in the present work in a mildly alkaline solution, it is reasonable to state that the critical value of [DKP]/[Cl^-] strongly depends on the solution pH and thus the higher concentration of hydroxyl groups can help to make an effective inhibition at a lower [DKP]/[Cl^-] ratio.

Dhouibi et al. [28] have also pointed to the cathodic inhibition of phosphate when [DKP]/[Cl^-] less than 0.6 due to a decrease in E_{corr} value with phosphate concentration; however, they have not found any evidence of passivation of metal surface. Nor have they offered any information about the change in the values of corrosion current density. These findings are similar to those obtained in the present work when [DKP]/[Cl^-] is less than 5.5. Therefore, a decrease in E_{corr} associated with an increase in i_{corr} can serve as an indication of an active state of corrosion not as a cathodic inhibition mechanism.

Table 3 shows that the greatest IE value (63%) is achieved at 11 mmol L^{-1} phosphate concentration. This value may induce a rather weak performance of phosphate in the case of the uniform corrosion. However, based on the polarization method, the short time of exposure as well as the forced condition by the application of high potentials far from the rest condition may affect the IE value

Table 3
Average value of polarization parameters for carbon steel in a 2 mmol L^{-1} chloride solution with different concentrations of DKP at 25 °C.

DKP concentration (mmol L^{-1})	Blank	7	11	17	23
[DKP]/[Cl^-]	0	3.5	5.5	8.5	11.5
Corrosion state	Active	Active-Passive	Passive	Passive	Passive
E_{corr}/E_{pass} (mV_{SCE})	−507 ± 11	−632 ± 12/−430 ± 11	−274 ± 8	−407 ± 9	−457 ± 11
i_{corr}/i_{pass} (μA cm^{-2})	8.9 ± 0.5	10.8 ± 0.5/30.6 ± 0.8	3.3 ± 0.4	5.2 ± 0.6	19.2 ± 0.5
β_c (mV/dec)	−495 ± 15	−253 ± 12	−246 ± 8	8235 ± 8	−228 ± 5
β_a (mV/dec)	211 ± 15	428 ± 10	–	–	–
E_{pit} (mV_{SCE})	–	−105 ± 15	81 ± 21	354 ± 28	467 ± 22
$E_{pit} - E_{pass}$ (mV_{SCE})	–	225 ± 26	355 ± 29	761 ± 37	924 ± 33
IE%	–	–	63	41	–

especially at the concentrations with a likelihood of passivation. This subject will be further discussed later using the other methods.

3.1.2. Electrochemical impedance spectroscopy

To further investigate the inhibition effect of phosphate on the corrosion behavior of carbon steel at open circuit potential (OCP), impedance spectra were registered at different concentrations of DKP. Prior to the impedance tests, OCP values were recorded for about 90 min (see Fig. 2), where a steady condition was achieved after about 60 min immersion time. The EIS diagrams in 2 mmol L^{-1} chloride solutions containing different concentrations of DKP are shown in Fig. 3.

For analyzing the EIS spectra, two equivalent circuits illustrated in Fig. 4 are used [2]. The circuit (a) with one time constant represents an active corrosion state in the solution free of phosphate. Circuit (b) with two time constants corresponds to the corrosion of carbon steel in the presence of phosphate when there is a likelihood of the formation of passive film on the metal surface [5]. In circuit (b), the external and internal circles are attributed respectively to the formation of passive film and corrosion phenomena at the metal/passive film interfacial. In these circuits, R_s represents the solution resistance, R_f is attributed to the ionic transfer resistance of solution through passive film pores and R_{ct} is the charge transfer resistance at metal/film interface. The elements of CPE_f and CPE_t correspond to the constant phase element of the passive film and metal/film interface, respectively. The constant phase element (CPE) is used instead of the capacitance element when the capacitive loop in the Nyquist plot is a depressed semicircle [29]. This mainly arises from the non-homogeneity or roughness of the metal surface [30,31]. The impedance of CPE is described by the following relation:

$$Z_{CPE} = \frac{1}{Y(\omega j)^n} \tag{2}$$

where Y is a pseudo-capacitance parameter (Ω^{-1} s^n cm^{-2}) and ω the angular frequency (rad/s). j defines the imaginary number ($\sqrt{-1}$) and n is the CPE exponent related to the geometry of surface. The ideal capacitance value (C) can be calculated as follows:

$$C = \left(Y/R^{n-1}\right)^{1/n} \tag{3}$$

Regarding this equation, the terms C_f and C_t correspond to the ideal capacitance of passive film and metal surface, respectively. The parameters n_f and n_t denote the power constant for passive film and metal/film interface, respectively.

The validity of the EIS data was checked using Kramers-Kronig transformation (K-KT) at the applied frequency range. For illustration, the K-KT and measured impedance data at 11 mmol L^{-1} DKP are presented in Fig. 5. The reliability of the EIS data with respect to the stability and causality was found.

The effect of DKP concentration on the characteristics of passive film including film resistance (R_f), film capacitance (C_f), and parameter n_f are presented in Fig. 6. It is obvious that the increase in DKP concentration up to 11 mmol L^{-1} is associated with a significant increase in R_f, a decrease in C_f and a slight increment of n_f. While further incorporation of DKP within the solution up to 23 mmol L^{-1} leads to a reverse trend of variations for these parameters which implies an increase in the porosity level of the passive film.

The greatest value of R_f at 11 mmol L^{-1} DKP can be attributed to the highest ion transfer resistance of the solution within the passive film pores. At the same time, the smallest value of C_f and the greatest value of n_f indicate the least amount of penetration of solution constituents within the passive film pores and the most structural compaction of the passive film, respectively.

Fig. 7 shows the effect of DKP concentration on the corrosion features in the metal/passive film interfacial. Addition of 7 mmol L^{-1} DKP within the solution is associated with a slight decrease in charge transfer resistance, R_{ct}, (from 2.59 to 1.68 kΩ cm^2), a significant increase of metal surface capacitance, C_t, (from 2 to

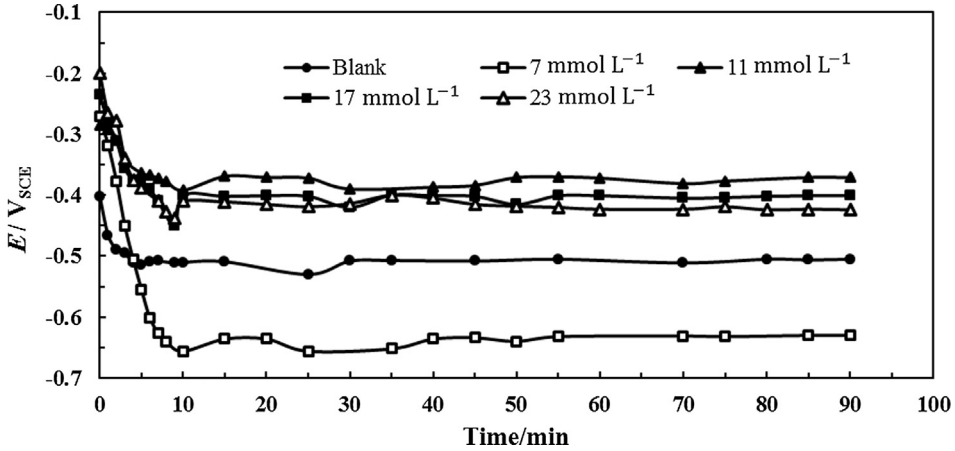

Fig. 2. Variation of OCP versus time at different concentrations of DKP for carbon steel in mildly alkaline solutions with 2 mmol L^{-1} chloride at 25 °C.

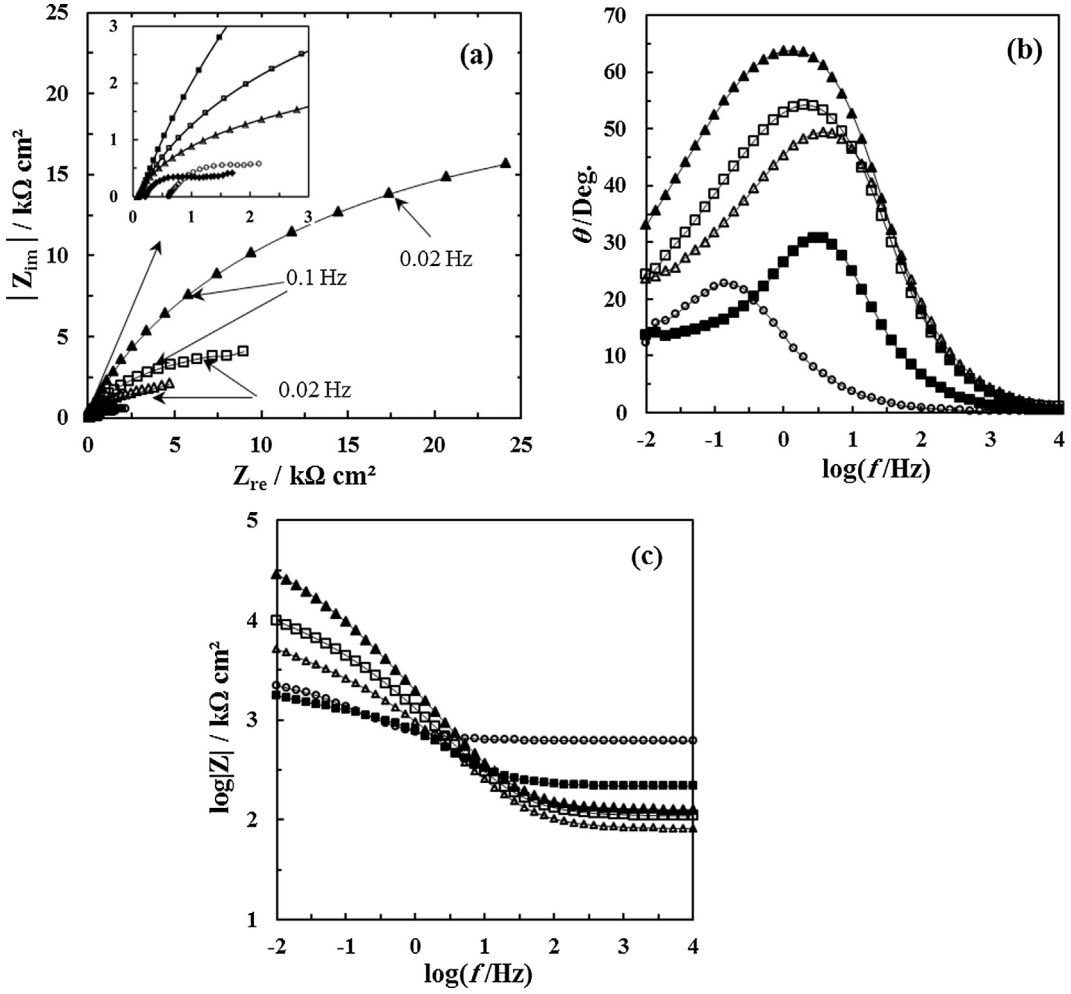

Fig. 3. Impedance spectra presented in the form of (a) Nyquist plot, (b) and (c) Bode plots for carbon steel in mildly alkaline solutions with 2 mmol L^{-1} chloride at different DKP concentrations: Blank (○), 7 mmol L^{-1} (■), 11 mmol L^{-1} (▲), 17 mmol L^{-1} (□), 23 mmol L^{-1} (Δ), fitting line (–) after 90 min immersion at 25 °C.

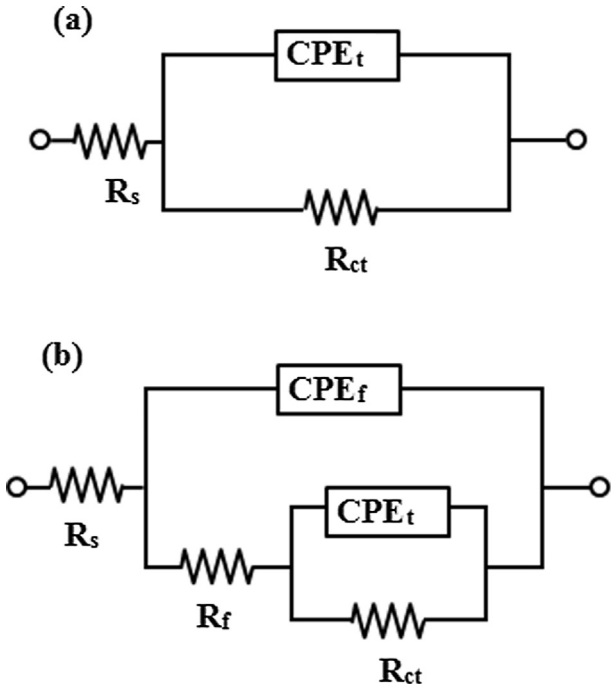

Fig. 4. Equivalent circuits used for analyzing the impedance data.

11 mF cm^{-2}), and an intensive decrease of parameter n_t. These variations support the fact that the dissolution of iron ions is stimulated in a 7 mmol L^{-1} DKP solution compared to the solution without DKP. Similar behavior was observed in the polarization test with an increase in i_{corr}.

It is obvious in Fig. 7 that the greatest value of R_{ct} and the smallest value of C_t are achieved at 11 mmol L^{-1} DKP, suggesting the best inhibition of DKP to the uniform corrosion. An increase in DKP concentration from 11 to 23 mmol L^{-1} causes steadily increment of C_t and decrease in both R_{ct} and n_t which induces the acceleration in the rate of metal dissolution. These behaviors are also in good agreement with the results obtained from the polarization test.

Comparing Figs. 6a and 7a, it can be found that the value of R_f is lower than that of R_{ct} at all DKP concentrations but it is not easy to distinguish on the Nyquist plots (Fig. 3a), especially at high DKP concentrations (≥11 mmol L^{-1}). This arises from the combination of two capacitive loops corresponding to the inner and outer circles of the electrical circuit shown in Fig. 4b due to the small difference in the value of time constants.

The inhibition efficiency (IE) was calculated through polarization resistance (R_p) as follows:

$$IE\% = \left(\frac{R_p - R_p^0}{R_p}\right) \times 100 \quad (4)$$

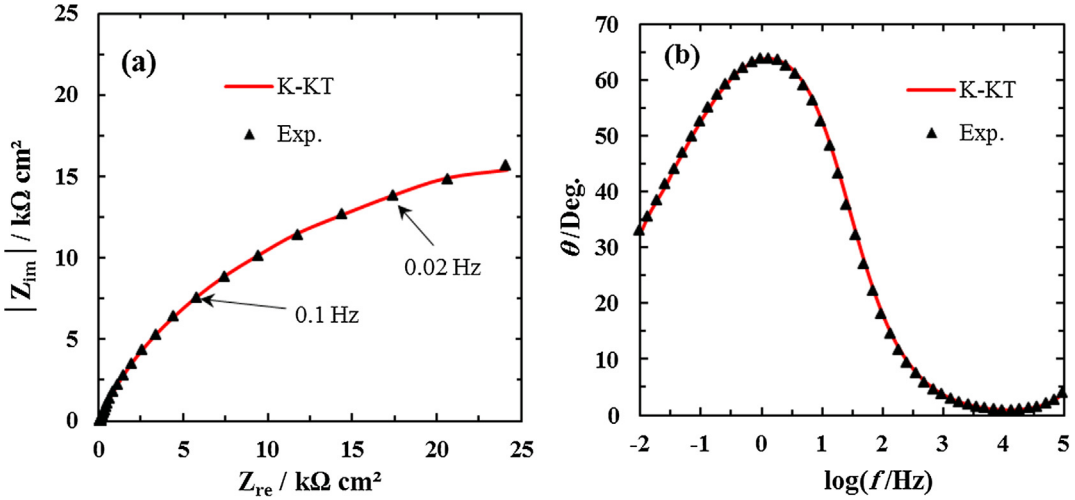

Fig. 5. Impedance data and Kramers–Kronig transformation (K-KT) in the form of (a) Nyquist, (b) Bode phase for carbon steel in a mildly alkaline solution with 2 mmol L^{-1} chloride + 11 mmol L^{-1} DKP at 25 °C after 90 min immersion.

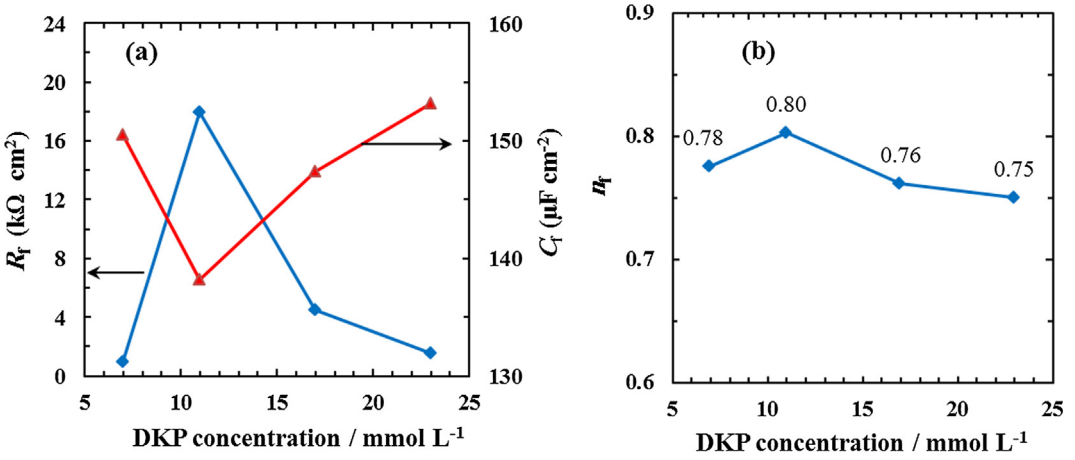

Fig. 6. Effect of DKP concentration on the (a) film resistance (R_f) and film capacitance (C_f), and (b) parameter n_f in mildly alkaline solutions with 2 mmol L^{-1} chloride at 25 °C.

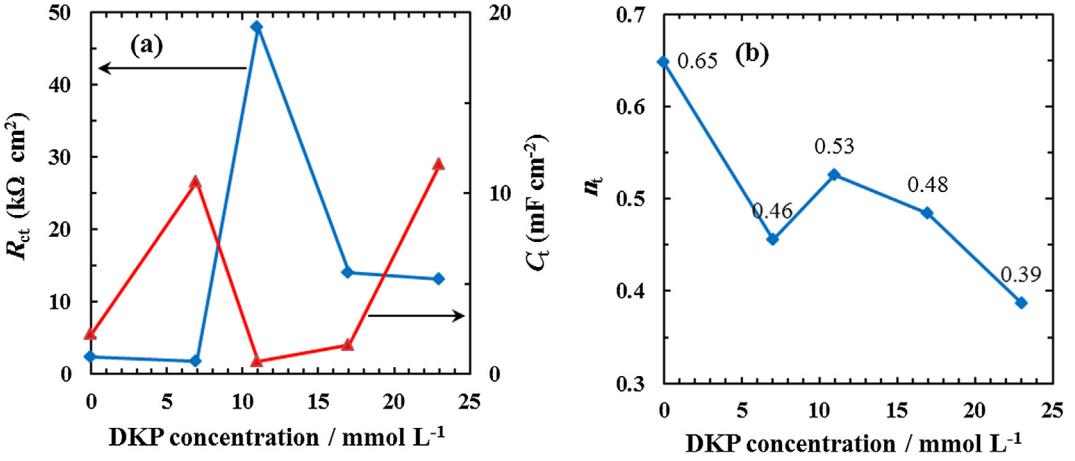

Fig. 7. Effect of DKP concentration on the (a) charge transfer resistance (R_{ct}) and capacitance (C_t) and (b) parameter n_t in mildly alkaline solutions with 2 mmol L^{-1} chloride at 25 °C.

where R_p and R_p^0 are the polarization resistance of carbon steel in the presence and absence of phosphate, respectively. Regarding the EIS method, it is known that $R_p = R_f + R_{ct}$. The values of R_p and IE at different DKP concentrations are given in Table 4.

Accordingly, the best inhibition efficiency (IE) is achieved at 11 mmol L^{-1} DKP ([DKP]/[Cl^-] = 5.5), while IE decreases when phosphate increases from 11 to 23 mmol L^{-1}. These variation trends are similar to those observed using the polarization test.

Table 4
Effect of DKP concentration on R_p and IE based on EIS data for carbon steel corrosion in mildly alkaline solutions with 2 mmol L^{-1} chloride at 25 °C.

DKP concentration (mmol L^{-1})	Blank	7	11	17	23
[DKP]/[Cl^-]	0	3.5	5.5	8.5	11.5
*R*p (kΩ cm^2)	2.59	2.43	65.91	18.55	12.51
IE%	–	–	96	86	79

However, it can be concluded that the IE values calculated using the EIS method at DKP concentrations between 11 and 23 mmol L^{-1} are significantly greater than those reported when using the polarization method in Table 3, which are similar to those reported before [26] and will be further evaluated by the weight loss method in the present work.

3.2. Effect of chloride concentration

Firstly, it should be noted that SCE reference electrode may contaminate the electrolyte by chloride diffusion and it may take on more significance in the case of a low chloride concentration involved here. This problem was examined through measuring the chloride concentration in a 2 mmol L^{-1} chloride + 11 mmol L^{-1} DKP solution before and after the polarization test. The results showed a less than 1 percent increase in chloride concentration probably due to the short time (between 15 and 40 min) that SCE electrode was exposed to the solution during the polarization test. This suggests that the side effect of SCE reference electrode can be ignored on the data obtained here; however, application of a chloride-free reference electrode would probably be a better option [13,26].

The effect of chloride contamination on the corrosion process of carbon steel in the presence of 11 mmol L^{-1} DKP was investigated using the potentiodynamic polarization method. The polarization curves in a 11 mmol L^{-1} DKP solution free of chloride and with different chloride concentrations including 1, 2, 3 and 5 mmol L^{-1} corresponds to the [DKP]/[Cl^-] ratios of 11, 5.5, 3.7 and 2.2, respectively, as shown in Fig. 8. The polarization parameters are presented in Table 5.

In the absence of chloride ions, the current density suddenly increases under high applied potential around 1.1 $V_{SCE,}$ which is attributed to the oxygen evolution process and not to the pitting occurrence on the passive film [32], while in the presence of chloride ions, the breakdown of passive layer takes place even at low chloride concentration. This behavior reflects the significant effect of chloride on the pitting process [33]. Unfortunately, at 5 mmol L^{-1} chloride concentration when [DKP]/[Cl^-] equals 2.2, the phosphate species are unable to passivate the steel surface at E_{corr} and a transient state from active to passive is observed at E_{pass} = −313 V_{SCE}. Therefore, [DKP]/[Cl^-] = 3.7 is a critical value; a similar value is also obtained as phosphate concentration varies.

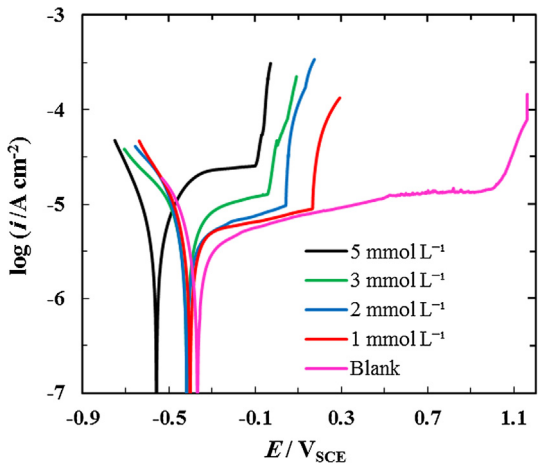

Fig. 8. Effect of chloride concentration on the potentiodynamic polarization curves for carbon steel in 11 mmol L^{-1} DKP solutions with 2 mmol L^{-1} chloride at 25 °C. Scan rate: 0.5 mV s^{-1}.

When the chloride concentration increases from 1 to 5 mmol L^{-1}, i_p markedly increases from 5.1 to 22.7 μA cm^{-2} and E_{corr} shifts towards the negative direction suggesting that chloride ions considerably activate the dissolution of iron ions [34]. Moreover, a decrease in both E_{pit} and passive region ($E_{pit}EE_{pass}$) as the chloride contamination increases as a result of the increase in the chloride attack on the passive layer at weak locations through more convenient adsorption and penetration, which leads to an easier breakdown of the passive film.

Some researchers have proposed that E_{pit} decreases with the logarithm of chloride concentration based on the following relation [35–37]:

$$E_{pit} = A - B\log[Cl^-] \quad (5)$$

where *A* and *B* are fitting parameters. The constant *A* shows the aggressiveness of the corrosive ions and the less positive value indicates the stronger effect at a given concentration [35]. The coefficient *B* depends on the electrolyte nature [38] and the type of electrochemical technique used [39].

Regarding Eq. (5), it is interesting to evaluate the effect of Cl^- concentration on the characteristics of the passive film including pitting potential (E_{pit}), passive potential (E_{pass}), and passive region ($E_{pit} - E_{pass}$). To this end, the mentioned parameters are plotted versus log [Cl^-] in Fig. 9 and have been satisfactorily fitted to the Eq. (5), as shown below:

$$E_{pit} = 0.18 - 0.39\log[Cl^-] \quad (6)$$

$$E_{pass} = -0.25 - 0.08\log[Cl^-] \quad (7)$$

$$E_{pit} - E_{pass} = 0.43 - 0.31\log[Cl^-] \quad (8)$$

Comparing Eqs. (6) through (8), the values of the parameter *A* obtained for the E_{pit} (Eq. (6)) is less positive than that reported by Ergun and Turan [40] in a phosphate solution (*A* = 0.35, *B* = 0.32), suggesting the higher aggressive electrolyte of the present work. In addition the values of the parameter *B* is close to each other which may be due to the nearly similar nature of the electrolytes composed of phosphate species in the form of HPO_4^{2-} ions.

In the case of E_{pass}, the less value of both parameters *A* and *B* can be considered as an indication of the higher ability of an inhibitor to make a passive layer on the metal surface in a corrosive environment, which has not been reported anywhere.

For the passive region ($E_{pit} - E_{pass}$), the higher value of parameter *A* suggests the increment of the passive region and its higher stability against the corrosive condition especially at low concentrations of corrosive ions, e.g. 1 mmol L^{-1} chloride in the present work. In the case of parameter *B* as the slope of the plot, the less value indicates the less deterioration effect of the increase in the corrosive ions concentration on the passive film.

The values of parameter *B* obtained by Eqs. (6) through (8) decrease with the following sequence: $B_{pit} > B_{pass\ region} > B_{pass}$. This sequence of variation implies the increase in chloride concentration provides the largest influence on E_{pit} and the least influence on E_{pass}. Since at each chloride concentration, the passive region is affected by the values of both E_{pit} and E_{pass}, parameters *A* and *B* calculated by Eqs. (6) through (8) can be related to each other by the following equations:

Table 5
Polarization parameters for carbon steel in 11 mmol L^{-1} DKP solutions in the absence and presence of different chloride concentrations at 25 °C.

Chloride concentration (mmol L^{-1})	0	1	2	3	5
[DKP]/[Cl^-]	–	11	5.5	3.7	2.2
Corrosion state	Passive	Passive	Passive	Passive	Active-Passive
E_{corr}/E_{pass} (mV_{SCE})	−250 ± 4	−255 ± 6	−274 ± 5	−290 ± 6	−557 ± 11/−313 ± 7
i_{corr}/i_{pass} (μA cm^{-2})	4.9 ± 0.1	5.1 ± 0.2	6.2 ± 0.4	8.4 ± 0.2	3.9 ± 0.1/22.7 ± 0.5
E_{pit} (mV_{SCE})	1080 ± 11	169 ± 22	75 ± 20	−30 ± 21	−95 ± 17
$E_{pit} - E_{pass}$ (mV_{SCE})	1330 ± 15	424 ± 28	349 ± 25	260 ± 27	218 ± 24

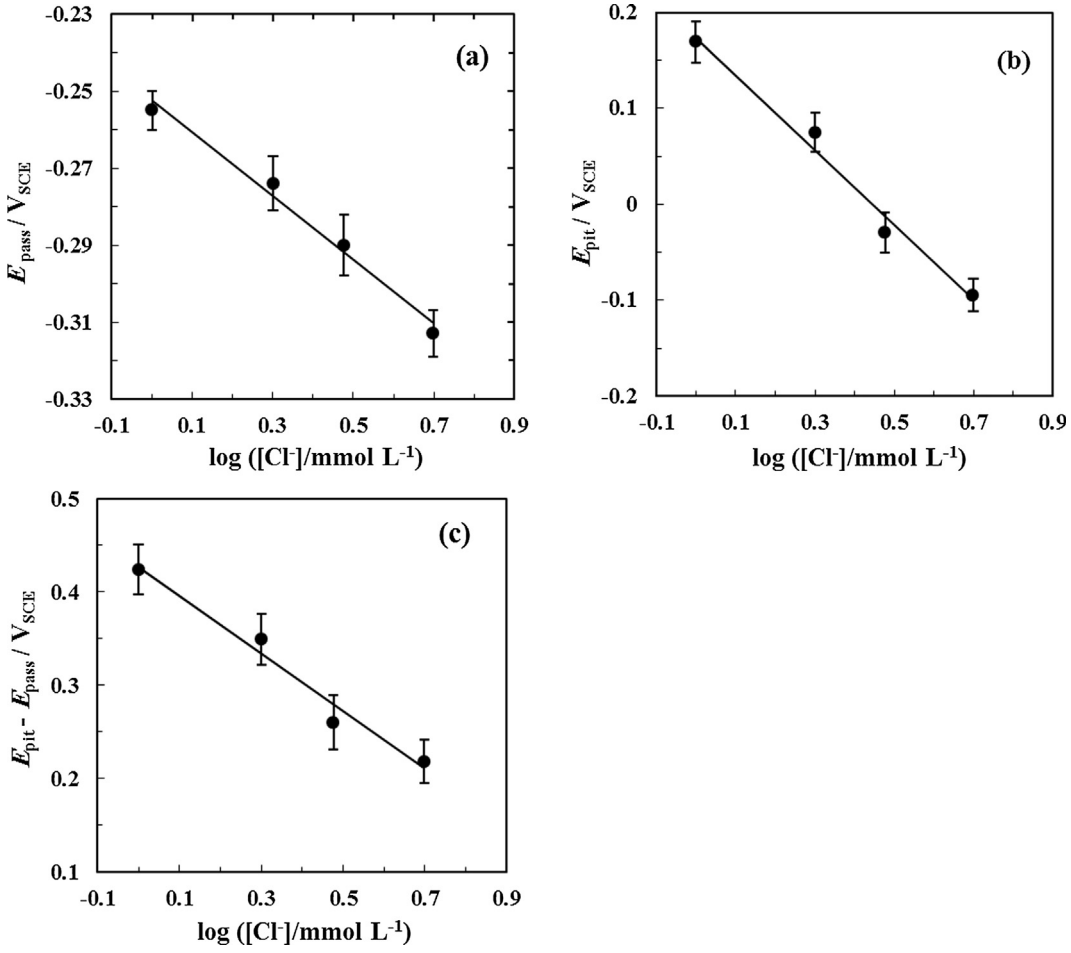

Fig. 9. Dependence of (a) E_{pass}, (b) E_{pit} and (c) E_{pit}- E_{pass} with logarithm of [Cl^-] for carbon steel in 11 mmol L^{-1} DKP solutions at 25 °C.

$$A_{\text{pass region}} = A_{\text{pit}} - A_{\text{pass}} \quad (9)$$

$$B_{\text{pass region}} = B_{\text{pit}} - B_{\text{pass}} \quad (10)$$

The influence of chloride concentration on the resistance of passive film can be briefly described as follows: the higher value of A and the lower value of B for the passive region will guarantee the higher resistance of the passive film to pitting corrosion.

3.3. Weight loss measurement

Evaluation of inhibition efficiency of DKP in the long term provides a reliable prediction of the inhibitor performance. The weight loss data for the ageing process of carbon steel samples in a 2 mmol L^{-1} chloride solution in the presence and absence of 11 mmol L^{-1} DKP are given in Table 6. The corrosion current density values were calculated using the Faraday's law as follows:

$$i_{\text{corr}} = \frac{(W_1 - W_2)\text{F}}{A\,t\,eq} \quad (11)$$

where W_1 is the weight of the specimen prior to immersion, W_2 is the weight of samples after immersion following thoroughly removing corrosion products from the surface of the specimen, F is Faraday's constant, A is the surface exposed to the corrosive media, t is the ageing time (45 days), and eq is the equivalent

Table 6
Weight loss data for carbon steel in a 2 mmol L^{-1} chloride solution in the absence and presence of 11 mmol L^{-1} DKP concentration after 45 days immersion.

Solution	W_1 (gr)	W_2 (gr)	i_{corr} (μA cm^{-2})	IE%
2 mmol L^{-1} chloride without DKP	39.312	39.121	16.980	–
2 mmol L^{-1} chloride + 11 mmol L^{-1} DKP	39.391	39.387	0.356	97.91

weight (27.92 g/mol for Fe). The percentage of inhibition efficiency of DKP at 11 mmol L^{-1} DKP concentration was calculated according to Eq. (1).

It can be found that the addition of 11 mmol L^{-1} DKP results in a high value (about 98%) of inhibition efficiency on the uniform corrosion; additionally, after cleaning the corrosion product, no sign of pitting was visually observed on the surface of the specimen. This information confirms the high efficiency of phosphate in protecting the carbon steel against both uniform and pitting corrosion.

The IE value calculated using weight loss is close to that obtained using the EIS method (97% in Table 4) and shows a great difference with that obtained using the polarization method (63% in Table 3). This finding suggests that the IE values obtained using the EIS method are more reliable and it can be concluded that DKP could efficiently protect the carbon steel against uniform corrosion even at high concentrations.

3.4. Surface analyses

3.4.1. SEM/EDS

The SEM images, EDS and Raman spectroscopy were employed to analyze the corrosion state and constituents of the passive film after anodic polarization till a sudden increase in the corrosion current was achieved. In this regard, the existence of passive region in the polarization curves guarantees the formation of a thick enough film and thus the elemental surveying will correspond to the film surface, rather than to the metal bulk.

The SEM image and EDS spectrum of carbon steel surface in a 2 mmol L^{-1} chloride + 11 mmol L^{-1} DKP solution are shown in Fig. 10. It is obvious that the breakdown of the passive film is associated with the formation of big pits. The EDS analysis in Fig. 10b reveals the presence of Fe, O, and P elements inside the pit, providing an evidence for the structure of the passive film that likely composed of iron oxides and iron phosphate complexes, which will be studied in detail using Raman analysis. Likewise, Fig. 10a shows the white color of corrosion products inside the pit indicating that phosphate species are particularly adsorbed on the weak points of the passive film in competition with chloride ions.

Fig. 11 shows the SEM and EDS of the morphology of carbon steel surface in a 2 mmol L^{-1} chloride + 23 mmol L^{-1} DKP solution. The SEM image (Fig. 11a) shows a large density and small size of white points on the metal surface, which can be considered as the weak points or even small pits created on the passive film which are not observable due to the accumulation of corrosion products mainly as iron phosphate complexes. Fig. 11a shows that the addition of high phosphate content ([DKP]/[Cl^-] = 11.5) diminishes the chloride attack on the metal surface compared to that observed in Fig. 10a at 11 mmol L^{-1} DKP concentration ([DKP]/[Cl^-] = 5.5). This observation is in keeping with the increase of E_{pit} with phosphate obtained using the polarization test in Table 3.

To further clarify the effect of chloride content, the SEM images and EDS analysis were recorded at the lower concentration of chloride (1 mmol L^{-1}), which are presented in Fig. 12. As can be seen, a decrease in chloride concentration from 2 mmol L^{-1} ([DKP]/[Cl^-] = 5.5) to 1 mmol L^{-1} ([DKP]/[Cl^-] = 11) increases the density of white points on the metal surface like that observed in Fig. 11a at a high phosphate concentration but at approximately the same [DKP]/[Cl^-] ratio. This implies that the ([DKP]/[Cl^-] ratio can be taken into account as an important factor in evaluating the degree of chloride attack onto the passive film. Moreover, Fig. 12b shows the EDS spectra recorded on an arbitrary area of metal surface where the high quantity of O and P elements suggests the thickening of the passive film as a result of an increase in the [DKP]/[Cl^-] ratio, which is similar to that obtained at 23 mmol L^{-1} in Fig. 11b.

Fig. 12c shows the SEM image taken on the white regions of the metal surface at a high magnification. It is obvious the existence of a pit in the white regions with much smaller size than that

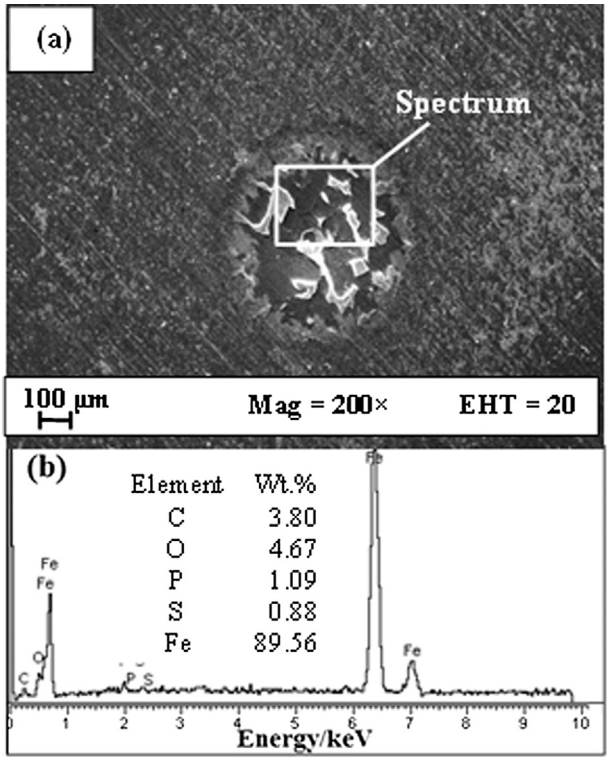

Fig. 10. SEM image (a) and EDS spectrum (b) of carbon steel surface after the anodic polarization test in a 2 mmol L^{-1} chloride + 11 mmol L^{-1} DKP solution at 25 °C.

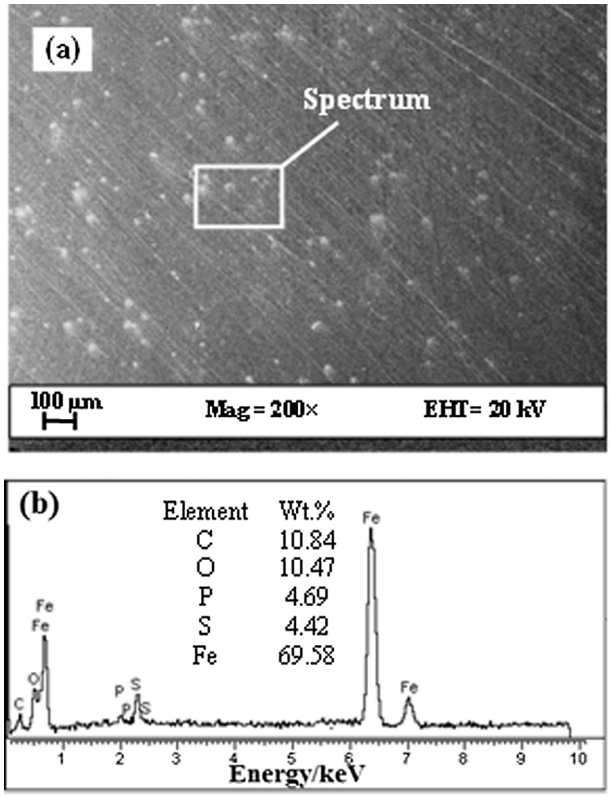

Fig. 11. SEM image (a) and EDS spectrum (b) of carbon steel surface after the anodic polarization test in a 2 mmol L^{-1} chloride + 23 mmol L^{-1} DKP solution at 25 °C.

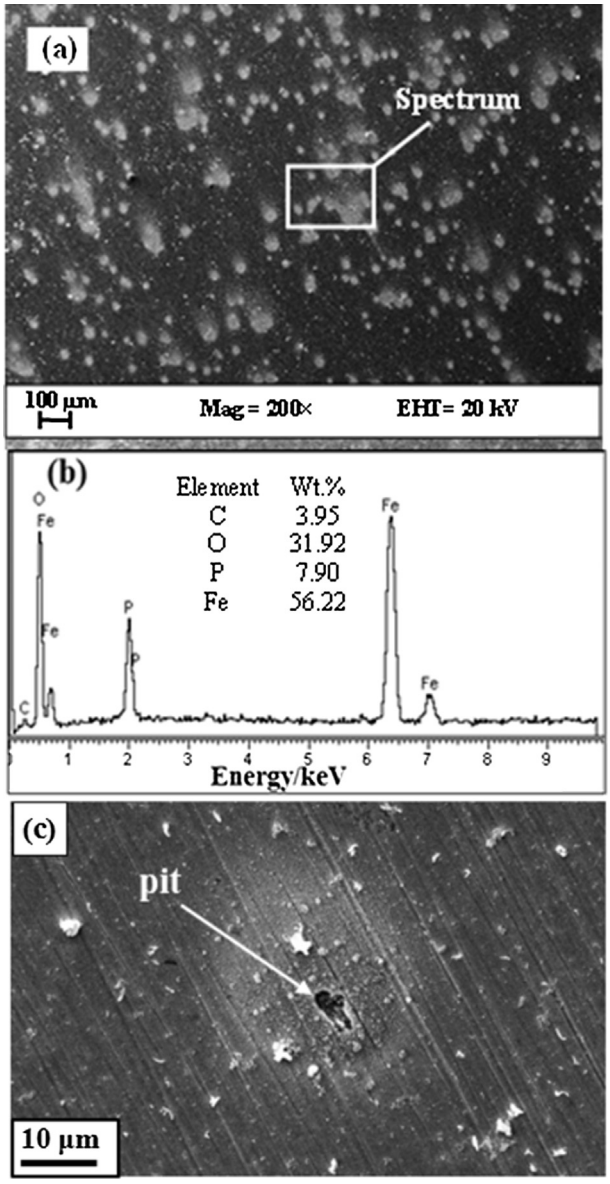

Fig. 12. SEM images at different magnifications (a and c) and EDS spectrum (b) of carbon steel surface after the anodic polarization test in a 1 mmol L^{-1} chloride + 11 mmol L^{-1} DKP solution at 25 °C.

observed in Fig. 10a. This indicates the higher [DKP]/[Cl^-] ratio causes higher protection against pitting growth.

3.4.2. Ex-situ Raman spectroscopy

Ex-situ Raman spectroscopy was used to characterize the constituents of the passive film in a 2 mmol L^{-1} chloride + 11 mmol L^{-1} DKP solution at 25 °C. To do this efficiently, Raman spectroscopy analysis was conducted on zones without pits and inside the pits induced by anodic polarization – the recorded spectra are shown in Fig. 13.

It is apparent that the Raman spectrum recorded inside the pits (Fig. 13a) is similar to that of the zones without pits (Fig. 13b); however, the spectrum corresponding to the passive film on the zones without pits has weaker intensity than pit zones probably due to the formation of a thin passive film or its disordered structure, which has been addressed previously [26,41].

Fig. 13a and b show two broad bands centered at about 989 and 850 cm^{-1} due to symmetric stretching modes and one at 1080 cm^{-1} due to antisymmetric stretching modes. These three bands are characterized by the presence of hydrogen phosphate (HPO_4^{2-}) anions. Also, three bands at about 412 (only in Fig. 13a), 550, and 935 cm^{-1} correspond to the presence of phosphate (PO_4^{3-}) anions. Such evidence demonstrates the incorporation of phosphate species (HPO_4^{2-} and PO_4^{3-}) into the passive film and inside the pits. The Raman analysis in the case of phosphate species is in good agreement with those reported earlier in the literature by Refait et al. [42], yohai et al. [5], and Simard et al. [43].

In addition, Fig. 13 shows the presence of magnetite (Fe_3O_4) at band about 680 cm^{-1}, maghemite (γ-Fe_2O_3) at four bands of about 360 cm^{-1}, 500 cm^{-1}, 650 cm^{-1} and 710 cm^{-1}, and α-Fe_2O_3 or at about 250 cm^{-1} and 614 cm^{-1} [26,44,45]. This information confirms the formation of iron oxide layers on the carbon steel surface.

3.5. Phosphate inhibition mechanism

3.5.1. In a mildly alkaline solution (pH = 8.8)

Regarding the obtained results, phosphate species could efficiently protect the carbon steel against corrosion in a mildly alkaline solution (pH about 8.8) contaminated with low chloride dosages through the anodic inhibition mechanism.

The surface analysis using SEM/EDX and Raman spectroscopy techniques support the view that the passivation of carbon steel surface in the presence of phosphate is attributed to the formation of a duplex layer, as illustrated in Fig. 15, which is in agreement with the results obtained earlier [11,15,46,47].

The inner layer consists of iron oxides mainly as Fe_3O_4 (magnetite) formed via a solid-state mechanism where Fe_3O_4 can be converted to γ-Fe_2O_3 (maghemite) in the presence of oxygen or under a high electric field [48,49].

In a mildly alkaline solution, phosphate species are mainly in the form of HPO_4^{2-}, adsorped on the weak points of the passive film following the reaction with the metal surface to form the iron phosphate complex of $FHPO_4$ via a dissolution-precipitation mechanism [3,47]:

$$Fe + HPO_4^{2-} \rightarrow FeHPO_4 + 2e^- \quad (12)$$

In the presence of oxygen and under a high electric field, $FHPO_4$ could be oxidized to a more stable form of $Fe_3(PO_4)_2$ or $FePO_4$ [15]. However, the probability of ferrous phosphate precipitation is greater than that of ferric phosphate because of its much greater pk_{sp} (32 for $Fe_3(PO_4)_2$ and 26 for $FePO_4$). In this regard, the phosphate layer could undergo the stabilization task of the inner layer of iron oxides against both uniform and pitting corrosion.

However, Table 3 shows that the addition of a high phosphate concentration, e.g. 23 mmol L^{-1} DKP, is associated with an increase in i_{pass}, likely due to the increment in the porosity level of the passive film as obtained by EIS (see Fig. 6). This concept can be interpreted as a competition process between phosphate species and hydroxyl groups to adsorb on the metal surface, whilst at a high phosphate concentration, the adsorption of hydroxyl groups decreases. In this situation, the contribution of ferrous phosphate layers in the structure of the passive film relative to that of iron oxides increases, as observed in the EDS analysis. This causes the increase in the porosity level of the passive film.

In the case of pitting corrosion, it is well known that there is a competition for adsorption on the metal surface between aggressive ions of chloride and those passivating ions of hydroxyl and phosphate [23,50]. On the one hand, chloride ions attack the weak points of the passive film and penetrate into the passive film. This induces the deterioration of the passive film and higher rate of metal dissolution [35]. On the other hand, hydroxyl groups and phosphate ions are adsorbed on the metal surface to stabilize the passive film against the aggressive ions. Under a high electric field, chloride ions penetrate into the passive film and cause the local-

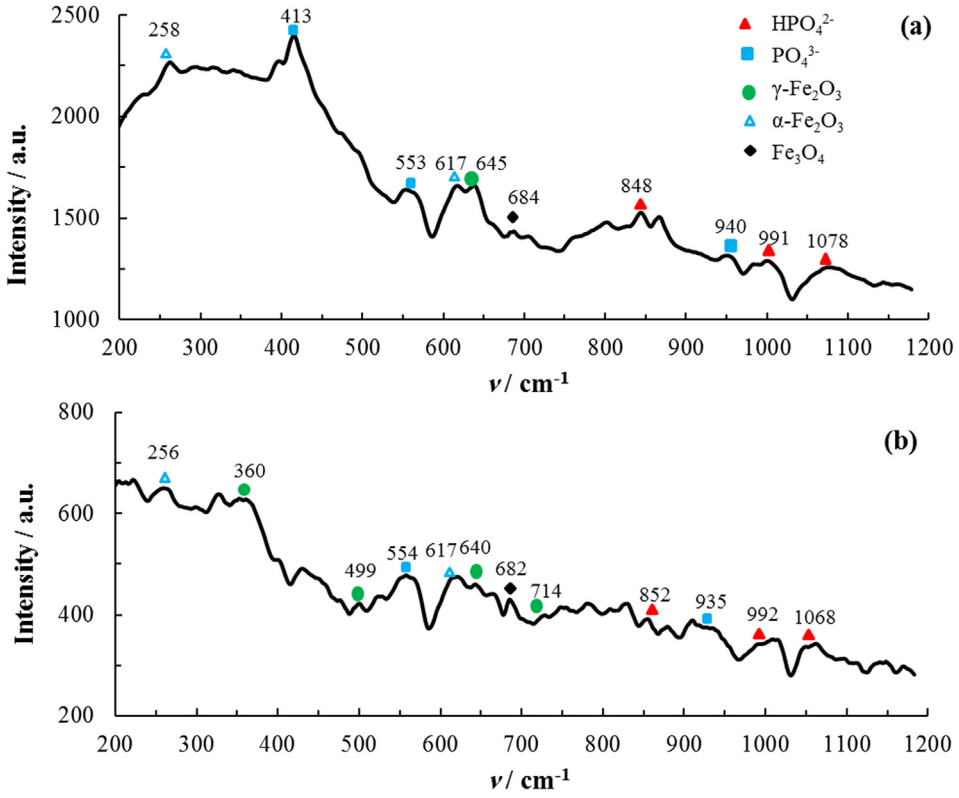

Fig. 13. Raman spectroscopy of carbon steel surface after the pitting process induced by the polarization test in a 2 mmol L^{-1} chloride + 11 mmol L^{-1} DKP solution at 25 °C: (a) inside the pits (b) zones without pits.

ized damage and breakdown of the passive film. In this situation, current density rapidly increases and pitting corrosion occurs.

In a mildly alkaline solution with 2 mmol L^{-1} chloride (pH = 8.8, $[Cl^-]/[OH^-] = 317$), an increase in the DKP concentration up to 23 results in a significant increase in E_{pit} (see Table 3), reflecting the important effect of phosphate in a synergistic behavior with hydroxyl groups to stifle the pitting corrosion and repair the weak points of the passive film.

SEM images and Raman spectroscopy analysis demonstrate the intensive adsorption of phosphate ions around either big or small pits on the passive film in competition with chloride ions to repair the defected points of the passive film [3].

3.5.2. In a highly alkaline solution (pH = 12)

Phosphate ions have been extensively used in a highly alkaline medium such as simulated pore solutions in concretes commonly contaminated with a high chloride dosage [13,14,27]. However, the low chloride contamination may also be detected during the early stages of exposure. This stage may last a long time depending on the concrete structure and electrolyte composition. To clarify the effectiveness of phosphate ions in a highly alkaline solution (pH 12) with low chloride contamination, polarization tests were carried out in a 2 mmol L^{-1} chloride solution in the absence and presence of 11 mmol L^{-1} DKP at pH 12 when $[Cl^-]/[OH^-] = 0.2$. The recorded polarization curves are shown in Fig. 14 and the main polarization parameters were calculated using the Tafel analysis, which are presented in Table 7.

As can be seen, when 11 mmol L^{-1} DKP is added to the solution, E_{pass} shifts towards the noble direction and i_{corr} markedly decreases. This offers a strong support for the fact that the anodic inhibition mechanism of phosphate can reduce the uniform corrosion of carbon steel in a highly alkaline solution, as reported by earlier other works, too [14,23,32].

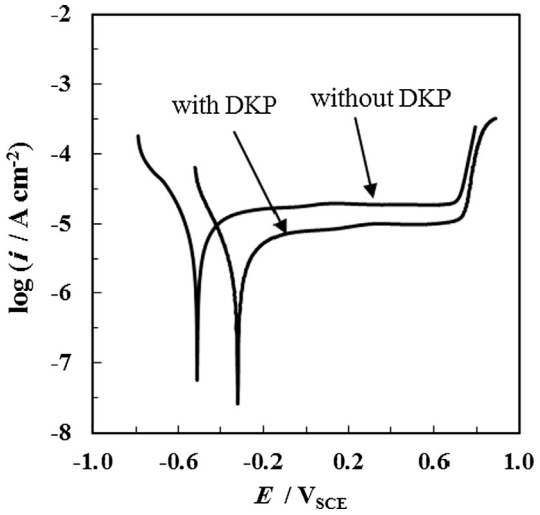

Fig. 14. Polarization curves for carbon steel in a highly alkaline solution (pH 12) with 2 mmol L^{-1} chloride in the absence and presence of 11 mmol L^{-1} DKP at 25 °C. Scan rate: 0.5 mV s^{-1}.

In the case of pitting corrosion, the sufficient high values of E_{pit} in the presence and absence of phosphate suggests that the pitting corrosion no longer occurs and, hence, the sudden increase in anodic current density is mainly attributed to the water oxidation phenomenon, as discussed earlier [24]. Likewise, no significant difference in the E_{pit} values is observed when DKP is added to the solution (see Table 7). Such a behavior clearly points to the predominant effect of hydroxyl groups on the chloride attack without the aid of phosphate species due to the high OH^- concentration relative to that of Cl^-.

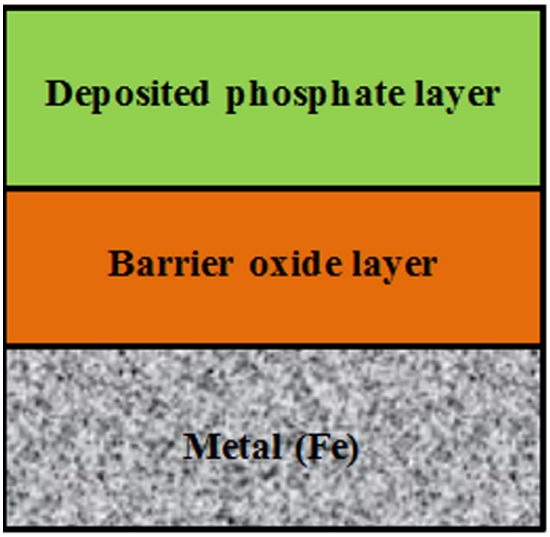

Fig. 15. Schematic illustration of the passive film formed on steel surface in a phosphate solution.

Table 7
The main polarization parameters calculated for carbon steel corrosion in a 2 mmol L^{-1} chloride solution in the absence and presence of 11 mmol L^{-1} DKP at pH 12 and 25 °C.

Solution	E_{pass} (mV_{SCE})	i_{pass} ($\mu A\ cm^{-2}$)	E_{pit} (mV_{SCE})
2 mmol L^{-1} chloride without DKP at pH 12	−512 ± 10	14.4 ± 0.3	711 ± 8
2 mmol L^{-1} chloride + 11 mmol L^{-1} DKP at pH 12	−323 ± 6	3.0 ± 0.4	720 ± 5

At pH = 12, PO_4^{3-} is the main form of phosphate species within the solution. The adsorption phenomenon following reaction of PO_4^{3-} with ferrous ions produces $Fe_3(PO_4)_2$ via a dissolution-precipitation mechanism as follows [5]:

$$3Fe + 2PO_4^{3-} \rightarrow Fe_3(PO_4)_2 + 6e^- \quad (13)$$

It was proposed that the precipitation of $Fe_3(PO_4)_2$ layer could stabilize the inner layer and repair its weak points against pitting corrosion, as discussed earlier [13]. However, here, in a highly alkaline solution ($[Cl^-]/[OH^-] = 0.2$) with a low concentration of chloride, phosphate is most effective against uniform corrosion.

4. Conclusion

The inhibitive behavior of phosphate with regard to carbon steel corrosion in both mildly and highly alkaline solutions with low levels of chloride contamination was studied using the electrochemical and surface analysis methods and the main results can be summed up as follows:

- In a mildly alkaline solution with low levels of chloride contamination (pH = 8.8, $[Cl^-]/[OH^-] = 317$), the $[DKP]/[Cl^-] = 3.7$ can be considered as a critical value at which a higher $[DKP]/[Cl^-]$ ratio is required to provide a reliable protection against both pitting and uniform corrosion through an anodic inhibition mechanism.
- In a mildly alkaline solution, when the $[DKP]/[Cl^-]$ ratio is greater than 3.7, a stable passive film was formed on the carbon steel surface at E_{corr}. The best inhibition against the uniform corrosion was achieved at 11 mmol L^{-1} DKP ($[DKP]/[Cl^-] = 5.5$) with respect to both the polarization and the EIS methods. Further addition of DKP up to 23 mmol L^{-1} causes an increase in the rate of uniform corrosion due to an increase in the porosity level of the passive film. In the case of pitting corrosion, an increase in DKP concentration up to 23 mmol L^{-1} is associated with a continuous increase in the resistance of the passive film by adsorption of phosphate species in the weak points of the passive film, which blocks the anodic sites.
- In a highly alkaline solution contaminated with low chloride (pH = 12, $[Cl^-]/[OH^-] = 0.2$), the presence of phosphate ions causes a decrease in the rate of the uniform corrosion by thickening the passive film as a result of precipitating the ferrous phosphate ($Fe_3(PO_4)_2$) layer. However, in the absence of phosphate, no pitting corrosion was identified using the polarization test even under a high electric field. It can be explained by the fact that the high concentration of hydroxyl groups relative to chloride ions causes a predominant effect to form a robust passive film, which in turn stops the pitting corrosion without the aid of phosphate.
- The SEM images taken from metal surface, EDS, and Raman spectroscopy analysis demonstrate the formation of a passive film with a duplex layer on the carbon steel surface including the inner layer of iron oxides (Fe_3O_4 or/and γ-Fe_2O_3) formed by a solid-state mechanism and the outer layer of iron phosphate complexes mainly as $FeHPO_4$, $Fe_3(PO_4)_2$, formed via a dissolution-precipitation mechanism. Moreover, it was apparent from SEM images that the phosphate adsorption phenomenon mostly takes place at weak points of the passive film where there is a serious competition between passivating and aggressive ions.

Conflict of interest

The authors herewith declare that there is no conflict of interest.

Acknowledgment

We would really like to thank Khorasan Razavi Gas Co. for providing us with laboratory facilities required for conducting the experiments for the purposes of the present study.

References

[1] S.M. Abd El Haleem, S. Abd El Wanees, E.E. Abd El Aal, A. Diab, Environmental factors affecting the corrosion behavior of reinforcing steel II. Role of some anions in the initiation and inhibition of pitting corrosion of steel in $Ca(OH)_2$ solutions, Corros. Sci. 52 (2010) 292–302.
[2] J. Shi, W. Sun, Effects of phosphate on the chloride-induced corrosion behavior of reinforcing steel in mortars, Cem. Concr. Compos. 45 (2014) 166–175.
[3] M. Reffass, R. Sabot, M. Jeannin, C. Berziou, P. Refait, Effects of phosphate species on localised corrosion of steel in $NaHCO_3$ + NaCl electrolytes, Electrochim. Acta 54 (2009) 4389–4396.
[4] N. Etteyeb, L. Dhouibi, H. Takenouti, M. Alonso, E. Triki, Corrosion inhibition of carbon steel in alkaline chloride media by Na_3PO_4, Electrochim. Acta 52 (2007) 7506–7512.
[5] L. Yohai, M. Vázquez, M. Valcarce, Phosphate ions as corrosion inhibitors for reinforcement steel in chloride-rich environments, Electrochim. Acta 102 (2013) 88–96.
[6] H. Kumar, V. Saini, D. Kumar, R. Chaudhary, Influence of trisodium phosphate (TSP) anti-salant on the corrosion of carbon steel in cooling water systems, Indian J. Chem. Technol. 16 (2009) 401–410.
[7] A. Douche-Portanguen, W. Prince, T. Lutz, G. Arliguie, Detection or quantitative analysis of a corrosion inhibitor, the sodium monofluorophosphate, in concrete, Cem. Concr. Compos. 27 (2005) 679–687.
[8] D.M. Bastidas, M. Criado, V. La Iglesia, S. Fajardo, A. La Iglesia, J. Bastidas, Comparative study of three sodium phosphates as corrosion inhibitors for steel reinforcements, Cem. Concr. Compos. 43 (2013) 31–38.
[9] A. Bastos, M. Ferreira, A. Simões, Corrosion inhibition by chromate and phosphate extracts for iron substrates studied by EIS and SVET, Corros. Sci. 48 (2006) 1500–1512.
[10] E. Alibakhshi, E. Ghasemi, M. Mahdavian, Corrosion inhibition by lithium zinc phosphate pigment, Corros. Sci. 77 (2013) 222–229.

[11] Z. Szklarska-Smialowska, R. Staehle, Ellipsometric study of the formation of films on iron in orthophosphate solutions, J. Electrochem. Soc. 121 (1974) 1393–1401.
[12] M. Pryor, M. Cohen, F. Brown, The Nature of the Films Formed by Passivation of Iron with Solutions of Sodium Phosphate, J. Electrochem. Soc. 99 (1952) 542–545.
[13] L. Yohai, M. Valcarce, M. Vázquez, Testing phosphate ions as corrosion inhibitors for construction steel in mortars, Electrochim. Acta 202 (2015) 316–324.
[14] H.B. Mansour, L. Dhouibi, H. Idrissi, Effect of Phosphate-based inhibitor on prestressing tendons corrosion in simulated concrete pore solution contaminated by chloride ions, Constr. Build. Mater. 171 (2018) 250–260.
[15] I.V. Sieber, H. Hildebrand, S. Virtanen, P. Schmuki, Investigations on the passivity of iron in borate and phosphate buffers, pH 8.4, Corros. Sci. 48 (2006) 3472–3488.
[16] T. Söylev, M. Richardson, Corrosion inhibitors for steel in concrete: State-of-the-art report, Constr. Build. Mater. 22 (2008) 609–622.
[17] M. Pryor, M. Cohen, The inhibition of the corrosion of iron by some anodic inhibitors, J. Electrochem. Soc. 100 (1953) 203–215.
[18] M. Pryor, M. Cohen, The mechanism of the inhibition of the corrosion of iron by solutions of sodium orthophosphate, J. Electrochem. Soc. 98 (1951) 263–272.
[19] R. Nishimura, M. Araki, K. Kudo, Breakdown of passive film on iron, Corrosion 40 (1984) 465–470.
[20] V. Ngala, C. Page, M. Page, Corrosion inhibitor systems for remedial treatment of reinforced concrete. Part 2: sodium monofluorophosphate, Corros. Sci. 45 (2003) 1523–1537.
[21] L. Dhouibi, E. Triki, M. Salta, P. Rodrigues, A. Raharinaivo, Studies on corrosion inhibition of steel reinforcement by phosphate and nitrite, Mater. Struct. 36 (2003) 530–540.
[22] D.M. Bastidas, M. Criado, S. Fajardo, A. La Iglesia, J.M. Bastidas, Corrosion inhibition mechanism of phosphates for early-age reinforced mortar in the presence of chlorides, Cem. Concr. Compos. 61 (2015) 1–6.
[23] H. Nahali, L. Dhouibi, H. Idrissi, Effect of Na_3PO_4 addition in mortar on steel reinforcement corrosion behavior in 3% NaCl solution, Constr. Build. Mater. 78 (2015) 92–101.
[24] H. Nahali, L. Dhouibi, H. Idrissi, Effect of phosphate based inhibitor on the threshold chloride to initiate steel corrosion in saturated hydroxide solution, Constr. Build. Mater. 50 (2014) 87–94.
[25] L. Yohai, W. Schreiner, M. Vázquez, M. Valcarce, Phosphate ions as inhibiting agents for copper corrosion in chlorinated tap water, Mater. Chem. Phys. 139 (2013) 817–824.
[26] L. Yohai, W. Schreiner, M. Vázquez, M.B. Valcarce, Phosphate ions as effective inhibitors for carbon steel in carbonated solutions contaminated with chloride ions, Electrochim. Acta 202 (2016) 231–242.
[27] H. Nahali, H.B. Mansour, L. Dhouibi, H. Idrissi, Effect of Na3PO4 inhibitor on chloride diffusion in mortar, Constr. Build. Mater. 141 (2017) 589–597.
[28] L. Dhouibi, E. Triki, A. Raharinaivo, G. Trabanelli, F. Zucchi, Electrochemical methods for evaluating inhibitors of steel corrosion in concrete, Br. Corros. J. 35 (2000) 145–149.
[29] H. Khani, R. Arefinia, Inhibition mechanism of nitrite on the corrosion of carbon steel in simulated cooling water systems, Mater. Corros. 69 (2018) 337–347.
[30] F. Bentiss, M. Lebrini, H. Vezin, F. Chai, M. Traisnel, M. Lagrené, Enhanced corrosion resistance of carbon steel in normal sulfuric acid medium by some macrocyclic polyether compounds containing a 1,3,4-thiadiazole moiety: AC impedance and computational studies, Corros. Sci. 51 (2009) 2165–2173.
[31] A. Pourghasemi Hanza, R. Naderi, E. Kowsari, M. Sayebani, Corrosion behavior of mild steel in H2SO4 solution with 1,4-di [1′-methylene-3′-methyl imidazolium bromide]-benzene as an ionic liquid, Corros. Sci. 107 (2016) 96–106.
[32] J.R. Génin, L. Dhouibi, P. Refait, M. Abdelmoula, E. Triki, Influence of phosphate on corrosion products of iron in chloride-polluted-concrete-simulating solutions: ferrihydrite vs green rust, Corrosion 58 (2002) 467–478.
[33] K.A.A. Al-Sodani, O.S.B. Al-Amoudi, M. Maslehuddin, M. Shameem, Efficiency of corrosion inhibitors in mitigating corrosion of steel under elevated temperature and chloride concentration, Constr. Build. Mater. 163 (2018) 97–112.
[34] M. Reffass, R. Sabot, C. Savall, M. Jeannin, J. Creus, P. Refait, Localised corrosion of carbon steel in $NaHCO_3$/NaCl electrolytes: role of Fe (II)-containing compounds, Corros. Sci. 48 (2006) 709–726.
[35] J. Soltis, Passivity breakdown, pit initiation and propagation of pits in metallic materials – Review, Corros. Sci. 90 (2015) 5–22.
[36] H.H. Strehblow, B. Titze, Pitting potentials and inhibition potentials of iron and nickel for different aggressive and inhibiting anions, Corros. Sci. 17 (1977) 461–472.
[37] Z. Szklarska-Smialowska, ZS-Smialowska, Pitting and crevice corrosion, NACE International, Houston, 2005.
[38] B.G. Ateya, F.M.A. Elnizamy, Kinetics of the hydrogen evolution reaction on mild steel electrodes in sulphuric acid, Corros. Sci. 20 (1980) 461–464.
[39] J.M. Kolotyrkin, Pitting corrosion of metals, Corrosion 19 (1963) 261t–268t.
[40] M. Ergun, A.Y. Turan, Pitting potential and protection potential of carbon steel for chloride ion and the effectiveness of different inhibiting anions, Corros. Sci. 32 (1991) 1137–1142.
[41] B. Díaz, S. Joiret, M. Keddam, X. Nóvoa, M. Pérez, H. Takenouti, Passivity of iron in red mud's water solutions Electrochim. Acta 49 2004 3039 3048.
[42] P. Refait, M. Reffass, J. Landoulsi, R. Sabot, M. Jeannin, Role of phosphate species during the formation and transformation of the Fe (II–III) hydroxycarbonate green rust, Colloids Surf, A 299 (2007) 29–37.
[43] S. Simard, M. Odziemkowski, D. Irish, L. Brossard, H. Ménard, In situ micro-Raman spectroscopy to investigate pitting corrosion product of 1024 mild steel in phosphate and bicarbonate solutions containing chloride and sulfate ions, J. Appl. Electrochem. 31 (2001) 913–920.
[44] A. Hugot-Le Goff, J. Flis, N. Boucherit, S. Joiret, J. Wilinski, Use of Raman spectroscopy and rotating split ring disk electrode for identification of surface layers on iron in 1M NaOH, J. Electrochem. Soc. 137 (1990) 2684–2690.
[45] M. Valcarce, C. López, M. Vázquez, The role of chloride, nitrite and carbonate ions on carbon steel passivity studied in simulating concrete pore solutions, J. Electrochem. Soc. 159 (2012) C244–C251.
[46] W. Kozlowski, J. Flis, An ellipsometric study of the effect of phosphate anions in borate solution on anodic films grown on iron, Corros. Sci. 32 (1991) 861–875.
[47] G. Vatankhah, H. Menard, L. Brossard, Effect of sulfate and chloride ions on the electrochemical behavior of iron in aqueous phosphate solutions, J. Appl. Electrochem. 28 (1998) 999–1004.
[48] T. Misawa, K. Hashimoto, S. Shimodaira, The mechanism of formation of iron oxide and oxyhydroxides in aqueous solutions at room temperature, Corros. Sci. 14 (1974) 131–149.
[49] W. Xu, K. Daub, X. Zhang, J.J. Noel, D.W. Shoesmith, J.C. Wren, Oxide formation and conversion on carbon steel in mildly basic solutions, Electrochim. Acta 54 (2009) 5727–5738.
[50] S.A.M. Refaey, Inhibition of steel pitting corrosion in HCl by some inorganic anions, App. Surf. Sci. 240 (2005) 396–404.